A&A 376, 124–135 (2001)
DOI: 10.1051/0004-6361:20010931

Astronomy & Astrophysics

Adaptive optics L-band observations of the Galactic Center region

Y. Clénet[1], D. Rouan[1], E. Gendron[1], J. Montri[2], F. Rigaut[3], P. Léna[1], and F. Lacombe[1]

[1] Observatoire de Paris, DESPA, 5 place Jules Janssen, 92190 Meudon, France
[2] ONERA, 29 avenue de la Division Leclerc, BP 72, 92322 Chatillon Cedex, France
[3] Gemini Observatory, 670 N. A'ohoku Place, Hilo, Hawaii, 96720, USA

Received 5 February 2001 / Accepted 20 June 2001

Abstract. L-band adaptive optics observations of the Galactic Center region have been performed in June 1999 and May 2000 at La Silla with the 3.6 m telescope, using the ADONIS adaptive optics system. In June 1999, we used a dedicated infrared wave-front sensor, RASOIR. This paper reports on the photometry and astrometry of more than 40 stars. Thanks to additional adaptive optics K-band observations made at CFHT, colour-magnitude diagrams have been constructed to identify individual sources with various types of stars known in this region (AGB, LPV, WC9, WN9/WN10, Ofpe/WN9, YSO). The so-called "cool slash" stars (Ofpe/WN9) appear to be numerous in the field and an estimation of the extinction coefficient towards the Galactic Center from the colours of these intrinsically weakly absorbed stars leads to $A_K = 2.7$, which is among the lowest published values.

Key words. instrumentation: adaptive optics – Galaxy: center – infrared: stars – extinction – stars: population

1. Introduction

Before the advent of speckle technique and adaptive optics in the 90's, the center of the Milky Way was the only galactic nucleus on which sub-parsec details could be reachable at near-infrared and infrared wavelengths and has been the subject of numerous studies at various wavelengths (see Genzel et al. 1994 for a review).

It was first in the millimeter range that a compact and luminous source, Sgr A*, assumed to be the actual nucleus of the Galaxy, was discovered by Balick & Brown (1974). Benefiting from much less extinction than in the visible and from the high angular resolution achievable in adaptive optics, near-infrared is well adapted to the study of the Galactic Center. In this wavelength domain, three major axes of research currently exist to understand the real nature of Sgr A* and its nearest environment, within a few arcseconds scale:

– Search for a counterpart to Sgr A*. This is essential to constrain the nature of the emission mechanism. Though, one had to face the insufficent resolution and the poor precision in the infrared/radio coordinates registration. Thanks to speckle or adaptive optics techniques, and after the detection of sources (SiO and H_2O masers) both at radio and infrared wavelengths (Menten et al. 1997), the error box around Sgr A* was drastically reduced. In K-band, Eckart et al. (1995) first reported the detection of an extended or multiple possible counterpart, called "Sgr A* cluster", with $m_K \approx 12$ in $1''$ aperture. Then, they found a possible unique counterpart, with a variable magnitude ($m_K \geq 16.3$ in August 1992, April 1994, May 1998; $m_K \approx 15$ in June 1996 and July 1997; see Genzel & Eckart 1999). In L'-band, Simons & Becklin (1996) reported the observation of a possible counterpart with $m_{L'} = 12.1$;
– Study of the nuclear stars dynamics. A compact massive source, lying at the center of the Galaxy, is commonly associated with Sgr A*. Derived from observations of radial velocity and proper motions of stars in the vicinity of Sgr A* (Genzel et al. 1996; Genzel et al. 1997; Ghez et al. 1998), the mass of this compact object, probably a black hole, was found to be of the order of $2.6 \times 10^6\ M_\odot$;
– Study of the stellar population. Determination of the age, mass and luminosity of the stars around Sgr A* is necessary to understand the history of the Galactic Center region. Photometric and spectroscopic studies of individual stars (Lebofsky et al. 1982; Blum et al. 1995; Krabbe et al. 1995; Najarro et al. 1997) show the presence of both late-type stars

Send offprint requests to: Y. Clénet,
e-mail: yann.clenet@obspm.fr

(giants and supergiants, detected by their CO absorption) and younger stars, exhibiting either HeI/HI lines (Wolf-Rayet, Ofpe/WN9) or a steep featureless reddened continuum (young stellar objects, dusty giants or Wolf-Rayet).

In this article, we present the results of two observing campaigns performed in L-band with the ESO adaptive optics system ADONIS. Those observations deal with the search for an infrared counterpart to Sgr A* and the study of the stellar population.

2. Observations and data reduction

2.1. 1999 campaign

ADONIS is the adaptive optics system installed on the ESO 3.6 m telescope at La Silla (Chile). It delivers diffraction-limited images in the near-infrared (Beuzit et al. 1997). Using a Shack-Hartman wave-front sensor, it usually analyzes the light at visible wavelengths, but during this observing run, we used RASOIR, a prototype of the infrared wave-front sensor of NAOS, the future adaptive optics system of the VLT (see Appendix A).

The science camera was COMIC, optimized for L- and M-band observations (Lacombe et al. 1998). The plate scale was 0.1 arcsec/pixel and the field of view $12.8'' \times 12.8''$.

The Galactic Center was observed from 20 June to 21 June, 1999. The night prior to the science run was used to set-up the system and to check the performance of the instrument. During this night, we observed two stars (BS 8477 and SAO 166058) in L-band under rather good seeing conditions (from $0.45''$ to $0.55''$). Each one was simultaneously used as a science and reference object. The first star was chosen rather bright ($m_K = 4.71$, Bouchet et al. 1991) whereas the second star had a K-band magnitude $m_K = 6.51$ (Le Bertre 1991) close to the one of IRS 7, the reference star later used for the Galactic Center observations.

During the two following nights, the Galactic Center region was observed in L-band by servoing on IRS 7. We used a classical chopping mode with a sky position $20''$ S, $10''$ E from the object position. The question of the sky position is delicate. Obviously, one can see in Fig. 1 that stars were present in this sky frame. Although we tried to choose a region devoid of stars, this is difficult given the stellar crowding and the limited throw of the chopping mirror ($30''$ maximum). In the following (Sect. 2.4), we show that the photometric errors stemming from this presence of stars in the sky frame were small. Individual frame integration time was 10 s.

For calibration stars (BS 5712, BS 8477), we used a triple chopping mode for the first one (sky position $10''$ N, $10''$ E from the star, integration time: 3 s) and a classical chopping mode for the second (sky positionned $20''$ S, $10''$ E from the star, integration time: 8 s).

To servo on the fainter stars (SAO 166058 and IRS 7), we had to lower the bandwidth of the adaptive optics servo loop, in particular the sampling frequency of the wave-front sensor, chosen equal to 40 Hz. Where as for the brightest, BS 8477, a larger sampling frequency (up to 60 Hz) could be used.

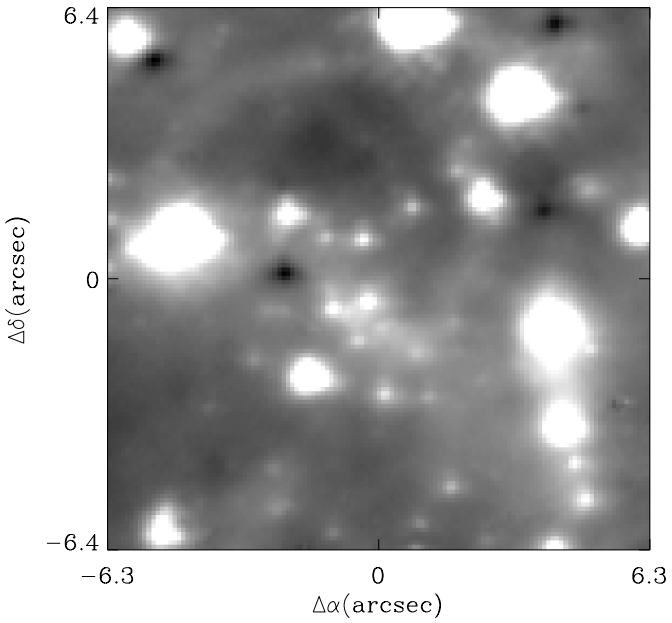

Fig. 1. 1999 L-band image of the Galactic Center region made with COMIC and RASOIR.

2.2. 2000 campaign

In 2000, the Galactic Center was observed from 20 to 22 May. For technical reasons, we could not use RASOIR and observed with the usual ADONIS visible wave-front sensor. The system was servoed on a star approximately $16''$ north and $15''$ east from Sgr A*. This star has a visible R-band magnitude of 13.8, which is at the limit of the ADONIS capabilities. The science camera was COMIC.

For the sky frame, given the limitation encountered during the 1999 run, we chose a region further away than for the first run by using 2MASS maps. We selected two regions free of sources near the Galactic Center, the first one beeing $12''$ north and $795''$ east from the reference star and the second $420''$ north and $690''$ west. The chopping mirror was not used and we rather performed nodding with the telescope (0101, 0: sky position, 1: object position), going alternatively to each sky position by spending approximatively 3 min on each field.

We also observed PSF calibration stars (Y4338 and Y3845, resp. $m_L = 5.12$, $m_L = 4.22$, Mc Gregor 1994) in chopping mode with a sky position $15''$ east from them. Density filters on the wave-front sensor were used to balance the adaptive optics correction between the calibration and Galactic Center fields.

2.3. Data reduction and performances

The data reduction applied to both runs was standard:

- bad pixels correction;
- sky substraction;
- flat field correction;
- recentering through cross-correlation techniques;
- straight co-addition of the resulting images.

Images obtained during the set-up night of the 1999 run demonstrated the ability of RASOIR to correct atmospheric turbulence. The performances obtained during this night, in terms of achieved angular resolution, are summarized in Table 1. With an average $FWHM$ of 0.26″ for BS 8477, the correction quality is close to the diffraction limit (0.20 arcsec in L-band for a 3.6 m telescope). In this particular example, the reduction of the sampling rate does not seem to have an impact on the angular resolution (see Table 1). When closing the loop on SAO 166058, the RASOIR detector received about five times less flux, leading to reduced performances.

During the 1999 run we obtained images of the Galactic Center region in L-band with a total integration time on source of 390 s. The images were poorly corrected due to unstable weather conditions (cirrus) and a worse seeing than during the set-up night. The average $FWHM$ of IRS 3 is 0.56″. Figure 1 gives the mean of all these images. One can note on this image the presence of residual triangular aberrations.

In 2000, we collected many more L-band images of the Galactic Center region, with a total integration time of 5368 s on source. Nevertheless, varying seeing conditions lead to dispersed $FWHM$: 1.6% of our images have a resolution below 0.4″, 13.8% are below 0.55″, 20% below 0.6″. Using drastic image selection criteria, we built the final image shown in Fig. 2, which has a resolution of 0.38″ for a total integration time of 88 s.

2.4. L-band photometry and astrometry

For both runs, photometry and astrometry of individual stars were done using the PSF-fitting procedure ALLSTAR from the DAOPHOT package (Stetson 1987). Because of the generally non photometric conditions during the runs, we have chosen to adjust our photometric zero-point with the photometry of Blum et al. (1996).

In their article Ott et al. (1999) gave a list of eleven stars that show no significant photometric variability in K-band over a period of nearly six years. Among these stars, we selected those which are clearly seen on our image (namely IRS 29N, IRS 33SE, IRS 16C, MPE +1.6-6.8, IRS 21, IRS 6E), and assumed that they are neither variable in L-band. The L-band zero point is fixed by computing for these stars the mean offset from our data to Blum et al. (1996). Photometric and astrometric results are given in Table 2.

The standard deviation of the difference between our photometry and the one of Blum et al. (1996), calculated for the six stars named above, is equal to 0.2 magnitudes in 1999 and 0.3 in 2000.

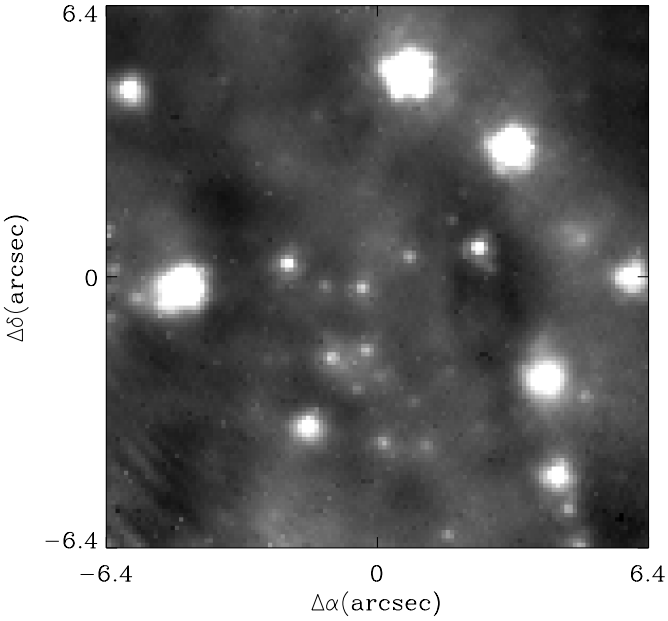

Fig. 2. 2000 L-band image of the Galactic Center region made with COMIC and ADONIS.

With rebinning methods, we achieved an estimated astrometric relative error of 0.03″.

More than 40 individual sources have been detected in a 12.5″ × 12.7″ region around Sgr A*. We estimate our limit magnitude to be around $m_L = 11$.

Photometry obtained in either run are similar except for a few sources. This demonstrates that 1999 results were marginally affected by the presence of few stars in the sky frame. Six sources (IRS 7SE, IRS 34W, IRS 16CC, MPE +1.0-7.6, IRS 33N and IRS 33SW) have an L-band magnitude difference larger than 0.5 between 1999 and 2000. It is difficult to invoke a possible variability of these stars without a longer follow-up of the region.

2.5. K-band image

In this article, we also use results of Galactic Center K-band observations obtained in July 1998 with PUEO, the CFHT adaptive optics system (Lai et al. 1997; Rigaut et al. 1998). The science camera used during this run was KIR (Doyon et al. 1998), with a field of view of 36″ × 36″ and a plate scale of 0.0348″ per pixel.

The resulting image is shown in Fig. 3 and reveals nearly 6400 stars. The clear Airy rings around them (see also Fig. 4) demonstrate that diffraction-limit has been reached. Astrometry and relative photometry were made with Starfinder (Diolaiti et al. 2000). To obtain the K-band magnitude of the sources, we used the same method as for the L-band: we calculated the K-band zero point using the photometry of the eleven reference stars of Ott et al. (1999). Results are given in Table 3.

Table 1. RASOIR performances.

Star name	K magnitude	Sampling frequency (Hz)	Seeing[a] ($''$)	$FWHM$ ($''$)
BS 8477	4.71[b]	60	0.45	0.26
		60	0.45	0.27
		50	0.55	0.26
		40	0.55	0.26
SAO 166058	6.51[c]	40	0.55	0.32
BS 5712	5.03[d]	40	0.6	0.51

[a] As given by the ESO seeing monitor;
[b] Bouchet et al. (1991);
[c] Le Bertre (1991);
[d] Thé et al. (1986).

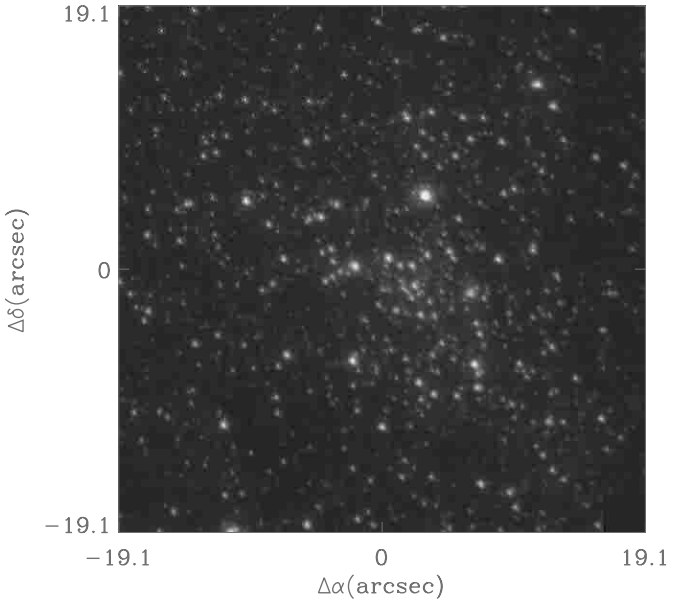

Fig. 3. K-band log (magnitude) scale image of the Galactic Center region, made with PUEO/KIR in 1998.

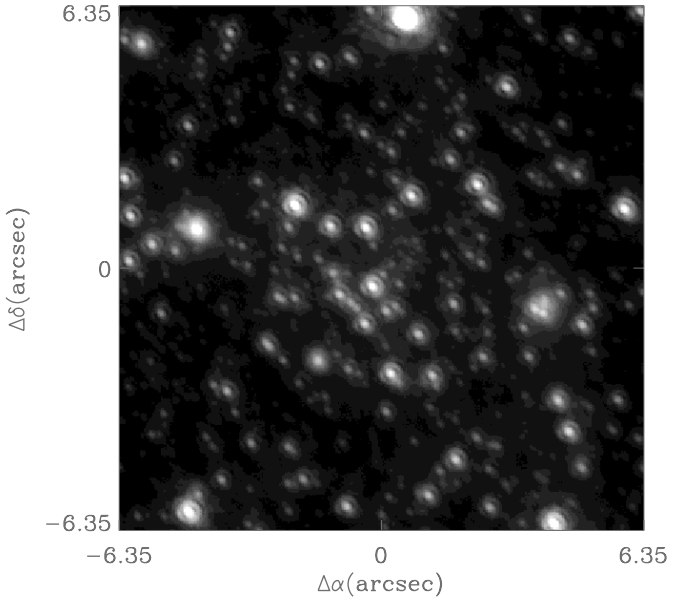

Fig. 4. Zoom of the precedent image on the region observed in L-band.

3. Analysis and discussion

3.1. Infrared counterpart of Sgr A*

The spectrum of Sgr A* is still badly known: identification at near and mid-infrared wavelengths of a counterpart to the radio source is not clear yet. As shown by Quataert et al. (1999), this is a crucial issue since luminosity upper limits imposed by infrared observations severely constrain the properties of accretion disk models.

On our 1999 and 2000 images, no conspicuous source has been observed at the location of Sgr A*. Assuming a K-band extinction coefficient of 3 and the A_L/A_K ratio derived from the extinction law of Rieke & Lebofsky (1985) ($A_L/A_K = 0.52$), our limit magnitude $m_L = 11$ leads to a deredenned flux density of 2.6 mJy. It corresponds to a luminosity $L_\nu = 2.0 \times 10^{20}$ ergs s^{-1} Hz^{-1} or $\nu L_\nu = 1.7 \times 10^{34}$ ergs s^{-1}. This upper limit is of the same order as the predicted value of the best model of Narayan et al. (1998): $\log(\nu L_\nu(\mathrm{erg\,s^{-1}})) \approx 34.2$. Thus, a much lower L-band luminosity would not be explained by this model.

3.2. Stellar population

Identifying the nature of stars populating the region of Sgr A* is of prime importance to derive the history of star formation in this region. Obviously, spectroscopy is the most efficient way to achieve it, but photometry and colour analysis may give some important clues.

3.2.1. What stars are observed?

A first remark is that no main sequence stars could be observed on our L-band images, despite the lower absorption suffered by near-infrared wavelengths. Assuming an absolute L-band magnitude about $M_L = -4.8$ (Allen 1973;

Table 2. 1999 and 2000 L-band photometry and astrometry.

ID	name	1999			2000		
		$\Delta\alpha^{a}$ ($''$)	$\Delta\delta^{a}$ ($''$)	L^{b}	$\Delta\alpha^{a}$ ($''$)	$\Delta\delta^{a}$ ($''$)	L^{b}
1	IRS 7	−2.86	4.55	4.9	−2.85	4.55	5.0
2	IRS 7E	1.49	4.33	10.2	1.51	4.35	10.5
3	IRS 10W	3.71	4.14	6.9	3.74	4.11	7.0
4	IRS 7W	−6.79	3.78	9.2	–	–	–
5	IRS 7SE	−0.57	3.53	9.7	−0.68	3.42	10.8
6	IRS 3	−5.31	2.78	5.5	−5.29	2.78	5.6
7	MPE –1.4–2.8	−4.19	1.70	9.5	–	–	–
8	IRS 29NE	−3.98	1.05	8.8	–	–	–
9	IRS 1NE	4.20	0.79	9.4	4.27	0.79	9.5
10	IRS 34W	−6.99	0.59	9.2	−6.95	0.57	8.7
11	IRS 29N	−4.51	0.39	7.2	−4.51	0.38	7.6
12	IRS 16NW	−2.84	0.15	9.0	−2.85	0.17	8.8
13	IRS 16NE	0	0	7.6	0	0	7.7
14	IRS 1C	4.06	−0.10	9.4	4.1	−0.13	9.2
15	IRS 6E	−8.14	−0.30	6.8	−8.13	−0.29	6.7
16	IRS 1W	2.44	−0.48	5.4	2.46	−0.50	5.6
17	IRS 16CC	−0.85	−0.56	8.8	−0.88	−0.55	9.5
18	IRS 16C	−1.71	−0.58	8.5	−1.76	−0.57	8.4
19	IRS 1NE(3)	–	–	–	3.47	−0.78	8.4
20	–	–	–	–	4.19	−1.27	9.2
21	IRS 16SW, IRS 16SW–W	−1.84	−2.05	8.2	−1.83	−2.06	8.4
22	IRS 16SW–E, MPE +1.6–6.8	−1.08	−2.21	8.3	−1.07	−2.24	8.1
23	IRS 35E	0.43	−2.25	10.4	0.49	−2.26	10.3
24	IRS 35W, IRS 16SE2	0.09	−2.29	10.6	0.06	−2.22	10.5
25	MPE −1.2–7.2	−3.65	−2.64	9.9	−3.78	−2.64	10.2
26	IRS 13E	−6.09	−2.67	6.5	−6.13	−2.65	6.7
27	–	−2.22	−2.67	8.9	−2.18	−2.65	9.3
28	MPE +1.0–7.6	−1.63	−2.85	8.8	−1.63	−2.89	9.3
29	IRS 13W	–	–	–	−6.98	−3.12	8.9
30	IRS 33N	−2.97	−3.17	8.9	−2.97	−3.27	10.0
31	MPE +3.4–8.2	0.69	−3.35	10.2	0.70	−3.53	9.4
32	IRS 21	−0.48	−3.80	6.9	−0.48	−3.85	7.1
33	IRS 33SE	−2.25	−4.17	8.9	−2.27	−4.23	8.7
34	IRS 33SW	−3.29	−4.24	9.9	−3.27	−4.32	9.1
35	IRS 2L	−6.34	−4.96	7.0	−6.37	−5.00	6.9
36	IRS 2S	−6.59	−5.79	8.5	−6.60	−5.76	8.6
37	–	0.25	−6.01	9.7	0.32	−5.97	9.1
38	IRS 20	−3.75	−6.31	9.1	−3.81	−6.42	9.1
39	–	−6.81	−6.65	8.4	−6.84	−6.61	8.6
40	–	−0.29	−6.82	9.2	–	–	–
41	MPE −0.6–11.9	−3.06	−7.18	10.2	–	–	–
42	MPE +1.4–12.2	−1.06	−7.41	10.1	–	–	–
43	IRS 9	2.88	−7.46	7.2	–	–	–
44	IRS 12N	−6.16	−7.91	8.0	–	–	–

[a] Offsets in arcseconds from IRS 16NE;
[b] Photometry calibrated with data from Blum et al. (1996, see text).

Table 3. K-band photometry.

ID	name	$\Delta\alpha^{a}$ ($''$)	$\Delta\delta^{a}$ ($''$)	K^{b}
1	IRS 7	–	–	6.6[c]
2	IRS 7E	1.57	4.17	11.39
3	IRS 10W	3.72	3.90	10.35
4	IRS 7W	−6.64	4.03	11.95
5	IRS 7SE	−0.60	3.41	11.22
6	IRS 3	−5.12	2.86	10.62
7	MPE −1.4–2.8	−4.01	1.75	11.75
8	IRS 29NE	−3.76	1.11	11.46
9	IRS 1NE	4.13	0.65	10.18
10	IRS 34W	−6.82	0.74	11.60
11	IRS 29N	−4.41	0.50	9.85
12	IRS 16NW	−2.82	0.23	9.89
13	IRS 16NE	0	0	8.75
14	IRS 1C	3.99	−0.26	10.37
15	IRS 6E	−7.98	−0.09	9.48
16	IRS 1W	2.38	−0.58	8.72
17	IRS 16CC	−0.86	−0.50	10.22
18	IRS 16C	−1.71	−0.54	9.55
19	IRS 1NE(3)	3.46	−0.94	10.74
20	–	4.02	−1.34	10.58
21	IRS 16SW, IRS 16SW–W	−1.87	−1.96	9.41
22	IRS 16SW–E, MPE +1.6–6.8	−1.09	−2.16	10.62
23	IRS 35E	0.39	−2.23	11.28
24	IRS 35W, IRS 16SE2	0.01	−2.24	11.82
25	MPE −1.2–7.2	−3.84	−2.38	11.46
26	IRS 13E1	−5.81	−2.49	10.53
26b	IRS 13E2	−6.00	−2.59	10.67
26c	IRS 13N	−6.04	−2.33	10.77
27	–	−2.20	−2.54	11.20
28	MPE +1.0–7.6	−1.68	−2.85	10.41
29	IRS 13W	−6.94	−2.89	10.85
30	IRS 33N	−2.99	−3.11	10.84
31	MPE +3.4–8.2	0.66	−3.37	10.97
32	IRS 21	−0.56	−3.75	10.55
33	IRS 33SE	−2.32	−4.07	9.86
34	IRS 33SW	−3.32	−4.11	10.82
35	IRS 2L	−6.37	−4.71	10.65
36	IRS 2S	−6.63	−5.47	10.31
37	–	0.16	−5.85	11.97
38	IRS 20	−3.89	−6.14	10.56
39	–	−6.93	−6.33	11.77
40	–	−0.20	−6.62	11.78
41	MPE −0.6–11.9	−3.22	−7.00	11.00
42	MPE +1.4–12.2	−1.25	−7.28	10.92
43	IRS 9	2.56	−7.41	8.66
44	IRS 12N	−6.27	−7.69	8.66

[a] Offsets in arcseconds from IRS 16NE;
[b] Photometry calibrated with data from Ott et al. (1999, see text);
[c] Photometry from CFHT AO image done in June 1996.

Table 4. $K-L$ magnitude and star identification.

ID	name	$K-L$[a]	identification
1	IRS 7	1.7	LPV
2	IRS 7E	1.2	Ofpe/WN9
3	IRS 10W	3.5	
4	IRS 7W	2.8	Ofpe/WN9-WN9-WN10
5	IRS 7SE	1.5	
6	IRS 3	5.1	YSO
7	MPE −1.4–2.8	2.3	AGB
8	IRS 29NE	2.7	WC9
9	IRS 1NE	0.8	
10	IRS 34W	2.4	Ofpe/WN9
11	IRS 29N	2.7	WC9
12	IRS 16NW	0.9	Ofpe/WN9
13	IRS 16NE	1.2	Ofpe/WN9
14	IRS 1C	1.0	
15	IRS 6E	2.7	WC9
16	IRS 1W	3.3	YSO
17	IRS 16CC	1.4	Ofpe/WN9
18	IRS 16C	1.1	Ofpe/WN9
19	IRS 1NE(3)	–	
20	–	–	
21	IRS 16SW, IRS 16SW–W	1.2	Ofpe/WN9
22	IRS 16SW–E, MPE +1.6–6.8	2.3	WC9
23	IRS 35E	0.8	
24	IRS 35W, IRS 16SE2	1.2	WC9
25	MPE –1.2–7.2	1.6	AGB
26	IRS 13E1	–	WN9–WN10
26b	IRS 13E2	–	
26c	IRS 13N	–	
27	–	2.3	
28	MPE +1.0–7.6	1.6	
29	IRS 13W	–	AGB
30	IRS 33N	1.9	
31	MPE +3.4–8.2	0.8	
32	IRS 21	3.7	YSO
33	IRS 33SE	1.0	Ofpe/WN9
34	IRS 33SW	0.9	AGB
35	IRS 2L	3.7	B[e]
36	IRS 2S	1.8	AGB
37	–	2.3	
38	IRS 20	1.5	
39	–	3.4	
40	–	2.6	
41	MPE –0.6–11.9	0.8	
42	MPE +1.4–12.2	0.8	
43	IRS 9	1.5	LPV
44	IRS 12N	0.7	LPV

[a] Calculated from Tables 3 and 2 (1999, L-band photometry).

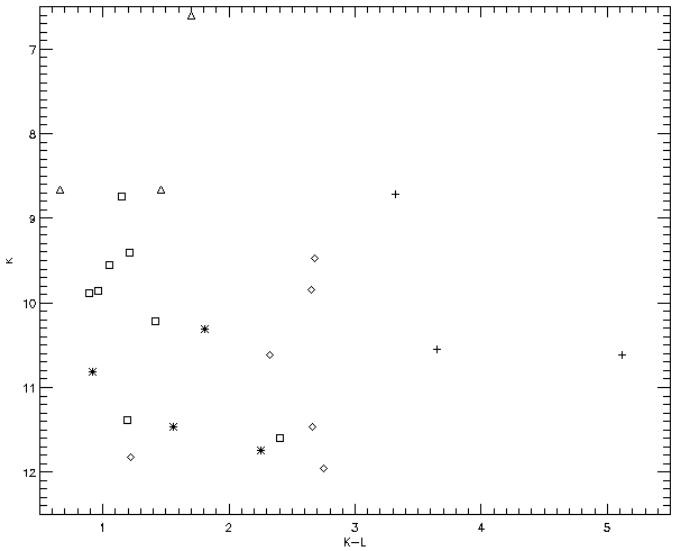

Fig. 5. Colour-magnitude diagram of stars already identified in literature. Single cross is for YSO, double cross for AGB, triangle for LPV, diamond for late-type Wolf-Rayet (WC9 and WN9/WN10) square for Ofpe/WN9.

Johnson 1966), a distance from the Galactic Center of 8.0 kpc (Reid 1993) and the same extinction coefficient and ratio as in Sect. 3.1, an O5 V star would be at $m_L = 11.3$, just above our limit magnitude: thus, only giants or supergiants could be seen.

3.2.2. Colour magnitude diagram of identified stars

Constructed from Tables 3 and 4, Fig. 5 presents a colour magnitude diagram of stars whose type has already been identified by spectroscopic means (Blum et al. 1995; Krabbe et al. 1995; Najarro et al. 1997). The offsets to apply in order to get a $(K-L)_0/M_K$ diagram are -1.4 along the x-axis and -17.5 along the y-axis.

The different types of identified stars can be classified as follows:

- *Late-type stars.* Identified due to CO absorption in the near-infrared spectra, they correspond to supergiants, asymptotic giant branch (AGB) stars, or long period variable (LPV) stars, the latter being bright thermally pulsating and variable AGB stars (Jones et al. 1983);
- *Emission line stars.* They were spectroscopically identified by the relative intensity of different lines (HeI, HeII, HI, CIII) emitted by strong stellar winds. They are blue supergiants in different evolution stages on the upper part of the Hertzprung-Russel diagram, including Ofpe/WN9, WN9 or WC9 stars. Ofpe/WN9 stars, also called "cool slash stars", are thought to be a precursor of Wolf-Rayet (WR) stars (Nota et al. 1996; Pasquali et al. 1997). WN9 and WC9 are late-type WR showing nitrogen and helium emission lines for the former, carbon and oxygen lines for the latter (Abott & Conti 1987);
- *Young stellar objects (YSO).* In the $12'' \times 12''$ region around Sgr A*, three stars have been proposed as hot young stars from their very red, featureless K-band spectra and from their strong emission at 10 μm (Krabbe et al. 1995).

Among the types of stars listed above, at least three of them could possess a dusty envelope: AGB, YSO and late WC stars. Thus, depending on the condition of obscuration, their colours could occupy a large range of values and overlapping may be expected.

Indeed, in the color-magnitude diagram, intersections exist between AGB and late-type Wolf-Rayet (WC9 and WN9/WN10 stars), but their positions in the diagram are not identical. Late-type WR stars spread along the K-band magnitude axis but are well located on the $K-L$ axis with an important infrared excess between 2.3 and 2.8 (except for IRS 35W with $K-L = 1.2$ and $m_K = 11.8$). These high reddening values are probably due to the dust shell that may surround late-type WR stars (Abott & Conti 1987; Cohen et al. 1991). On the other hand, AGB stars appear to be widespread along the $K-L$ axis, probably corresponding to the range of their envelope opacities, and less scattered on the K-band magnitude axis.

YSO are at the extreme right of the diagram with the largest $K-L$ colours and have no intersection with AGB or late-type WR. Their red spectrum and infrared excess are the signature of a dusty envelope or a possible accretion disk. Their colours vary from $K-L = 3.3$ to $K-L = 5.1$, which indicates a large range of obscuration.

LPV stars occupy the upper part of the diagram. Two of them (IRS 7 and IRS 9) have almost the same $K-L$ colour (around $K-L = 1.6$) showing an infrared excess probably due to the dust shell around AGB stars. The last one (IRS 12N) has a $K-L$ colour of 0.7, contrasting with the two others. Its intrinsic colour would then be equal to -0.7, a peculiar value for a star belonging to a class of dusty stars. An explanation could be its closeness to the lower border of our image. Then the derivation of its L-band magnitude by ALLSTAR may have been biased.

Ofpe/WN9 stars seem to have an homogeneous location on the $K-L$ axis (IRS 34W excepted), but their scattering along the K-band magnitude axis is important. These stars are the bluest of the region.

To give a comparison with the stars colours we present in this article, late-type M giants of the Baade's window, with an intrinsic $(K-L)_0$ colour around 0.3–0.4 (Frogel & Whitford 1987), would have an observed colour of 1.7–1.8 (always assuming $A_K = 3$ and $A_L/A_K = 0.52$).

3.2.3. Possible identification of stars

In Fig. 6 are superimposed stars that have not been identified yet. Many of them are placed in the lower left part of the diagram. According to the above description, they could either belong to the Ofpe/WN9 class or to the AGB class. Though, the stars with lower colour index may more probably pertain to the first one.

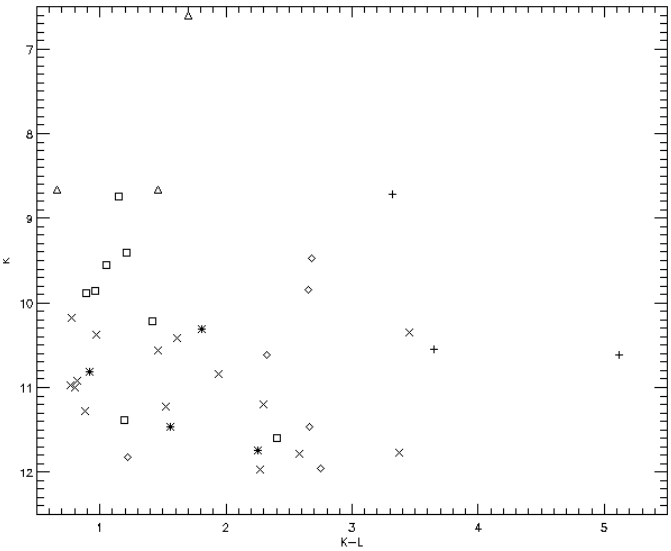

Fig. 6. Colour-magnitude diagram of identified and unidentified stars. Tilted single cross is for unidentified stars. See Fig. 5 for the identified stars symbols.

Three stars are located at the intersection of AGB and late-type WR domains and could belong to any of those two classes: ID#37 ($K-L = 2.3$, $K = 11.97$), ID#40 ($K-L = 2.6$, $K = 11.78$) and ID#27 ($K-L = 2.3$, $K = 11.2$).

Two stars possess an important $K-L$ excess: IRS 10W ($K-L = 3.5$, $K = 10.35$) and ID#39 ($K-L = 3.4$, $K = 11.77$). The former is really in the YSO domain and should belong to this class. The latter possesses a K-band magnitude similar to AGB stars and the same kind of colour excess as YSOs. It is then difficult to ascertain to which of those two classes it pertains.

Other YSOs may be present in the "IRS 13 complex". The PUEO K-band image (Fig. 4) cleary shows that IRS 13E is not a single star. It splits into at least three components, called IRS 13E1, IRS 13E2 and IRS 13N (see Table 3). These stars have about the same K-band magnitude (resp. 10.53, 10.67, 10.77). Our L-band images do not have enough resolution to distinguish these components: the largest distance between these three stars is $0.28''$. We observe a sole star with $m_L = 6.5$ in 1999 ($m_L = 6.7$ in 2000). Let us consider that, as in K-band, they all have about the same L-band magnitude, which would lead to the least $K-L$ values. Thus, the L-band magnitude of each component should be around 7.7. This leads to a minimum $K-L$ colour around 3.0 (with a mean K-band magnitude $m_K = 10.66$). Placed in our magnitude-colour diagram, this couple of values would match the YSO location. This could be all the more true if one choose a non uniform L-band magnitude distribution. The infrared colour excess would be even larger for at least one component of the IRS 13 complex.

To compare Galactic Center YSOs to other well studied YSOs, we have extended the YSO photometry work made by Blum et al. (1996) in the K- and H-band to the L-band. To make this comparison, we applied different corrections upon the YSO published photometry: corrections for the distance and for a foreground extinction towards the Galactic Center (assuming $A_K = 3$). Eventually, to substract a foreground extinction from a molecular cloud surrounding the YSO, we made the two same extreme assumptions as Blum et al. (1996): if the YSO is intrinsically red, all the $K-L$ colour is due to the YSO itself; if the YSO is intrinsically blue, all the $K-L$ colour is due to the surrounding cloud. Results are given in Table 5.

This L-band YSO study tends to confirm the conclusion made by Blum et al. (1996): Galactic Center YSO colours are both instrinsic and due to redenning, though, the trend seems to favor more the first assumption rather than the second. Intrinsic reddening would well account for the $K-L$ colour of the Galactic Center YSOs but they would appear a little too faint. On the other hand, intrinsically blue YSOs would have far too low colours and would be too bright.

Photometry at a third wavelength (H-band or M-band) and colour-colour diagrams would help refining the analysis above. Near-infrared spectroscopy at high angular resolution of still ambiguous stars, searching for the features listed more above, should definitely clear up the remaining ambiguities.

3.3. Extinction towards the Galactic Center

The K-band extinction towards Sgr A* given in the literature varies from 2.7 to 3.6 with important standard deviation errors. The different methods followed until now to calculate these values are presented in Rieke et al. (1989).

Though, for the bluer stars we observed, these values correspond to very negative intrinsic colours. If several physical processes lead to the reddening of intrinsic colours, it is very difficult to make them bluer. If one considers -0.2 as the lowest acceptable value for $(K-L)_0$, adopts a median value of 3 for the absorption coefficient in K-band and chooses the extinction law of Rieke & Lebofsky (1985), it comes that $K-L$ must be larger than 1.2. Actually, we found several unidentified stars with a $K-L$ colour below 1.2 (IRS 1NE, IRS 1C, IRS 35E, MPE +3.4–8.2, MPE –0.6–11.9, MPE +1.4–12.2) and also already identified stars: mainly Ofpe/WN9 (IRS 16NW, IRS 16C, IRS 33SE, IRS 7E, IRS 16NE, IRS 16SWW), and, surprisingly, an AGB (IRS 33SW) and a WC9 (IRS 35W) as well.

If we then consider that the lowest $K-L$ observed values correspond to the lowest $(K-L)_0$ acceptable value (-0.2), we find a quite weak extinction coefficient: $A_K = 2.1$. But this value would only be representative of the wings of a distribution whose mean value is greater. A better way to determine the reddening to the Galactic Center region may be to regard the bluer stars (i.e. Ofpe/WN9 class) as the most suitable estimator, since those stars should suffer the least intrinsic reddening. Excluding IRS 34W, whose behavior deviates from the majority, the Ofpe/WN9 mean infrared colour

Table 5. Young Stellar Object photometry.

YSO name	Observed (Observed YSO at 8 kpc)[a]		Redenned (Red YSO + GC extinction)[b]		Redenned (Blue YSO + GC extinction)[c]		References
	K_1	$(K-L)_1$	K_2	$(K-L)_2$	K_3	$(K-L)_3$	
CRL 2591	9.9	4.9	12.9	6.3	2.4	1.4	1
CRL 2059	8.2	2.6	11.2	4.0	5.6	1.4	2
CRL 490	10.1	2.8	13.1	4.2	7.1	1.4	1
CRL 989	9.6	2.1	12.6	3.5	8.1	1.4	3
W33A	10.5	3.8	13.5	5.2	5.4	1.4	4
S140/IRS 1	10.7	2.9	13.7	4.3	7.5	1.4	1, 5
CRL 961	10.7	2.5	13.7	3.9	8.3	1.4	2
NGC 7538/IRS 9	10.9	4.6	13.9	6.0	4.0	1.4	6
MonR2/IRS 3	10.5	4.1	13.5	5.5	4.7	1.4	7
BN	11.1	3.7	14.1	5.1	6.2	1.4	8
S255/IRS 1	11.6	4.1	14.6	5.5	5.8	1.4	9

[a] Observed K-band magnitude, corrected to a Galactic Center distance of 8 kpc. No reddening correction.
[b] Predicted K-band magnitude and $K-L$ colour of intrinsically red YSO at the Galactic Center: the intrinsic $K-L$ colour of the YSO is supposed equal to its observed $K-L$ colour and no correction is applied for the extinction in its surrounding cloud. We assumed $A_K = 3$ and $E(K-L) = 1.4$. $K_2 = K_1 + A_K$ and $(K-L)_2 = (K-L)_1 + E(K-L)$.
[c] Predicted K-band magnitude and $K-L$ colour of intrinsically blue YSO at the Galactic Center: the intrinsic $K-L$ colour of the YSO is supposed equal to 0 and the observed $K-L$ colour is used to correct for extinction in its surrounding cloud. We assumed $A_K = 3$ and $E(K-L) = 1.4$. $K_3 = K_1 + A_K.(1 - \frac{(K-L)_1}{E(K-L)})$ and $(K-L)_2 = E(K-L)$.
References for *K* and *L* photometry: (1) Noguchi et al. (1993); (2) Allen et al. (1977); (3) Merrill & Stein (1976); (4) Evans et al. (1979); (5) Evans et al. (1989); (6) Werner et al. (1979); (7) Manchado et al. (1989); (8) Lonsdale et al. (1982); (9) Evans et al. (1977).
Distances for all sources are from Wynn-Williams (1982).

is $\langle K-L\rangle_{\mathrm{Ofpe/WN9}} = 1.1$. Assuming $(K-L)_0 = -0.2$ and the extinction law of Rieke & Lebofsky (1985), this leads to $\langle A_K\rangle_{\mathrm{Ofpe/WN9}} = 2.7$.

This value is very close to $A_K = 2.8$, the mean extinction toward the inner bulge found by Davidge (1998). Thus, larger values of A_K found in the literature could be biased because of intrinsic reddening, or local effects (dusty clouds in the line of sight or shells surrounding the stars), or confusion due to crowding.

A different way to correct the very negative intrinsic colors would be to adopt another extinction law. From hydrogen recombination lines measurements, Lutz et al. (1996) found a A_L/A_K ratio of 0.58. Combined with a median value of $A_K = 3$, $\langle K-L\rangle_{\mathrm{Ofpe/WN9}} = 1.1$ would correspond to $\langle (K-L)_0\rangle_{\mathrm{Ofpe/WN9}} = -0.2$. The bluest stars would then belong to an acceptable intrinsic colors domain. This would suggest that the extinction law of Lutz et al. (1996) better describes the Galactic Center in L-band than the Rieke & Lebofsky (1985) extinction law, usually adopted in K-band.

4. Conclusions

We have presented L-band adaptive optics observations of a $13'' \times 13''$ region around Sgr A* obtained with ADONIS at La Silla in June 1999 and May 2000.

During the 1999 run, ADONIS was fitted with a new infrared wave-front sensor (IRWFS), RASOIR, originally made to prove the feasibility and the interest of wave-front sensing in the infrared. Results obtained during the first night seem promising for the NAOS IRWFS. During the second run, we used the usual ADONIS visible wave-front sensor.

For both runs, the correction on the Galactic Center field was not optimal: because of unstable weather conditions in 1999 and because of the distance between reference and object sources in 2000. Moreover, in both cases, we were guiding with a source at the limit of instrument capabilities. Thus, we cannot conclude, for the particular case of the Galactic Center region, which solution is the most appropriate; is it an infrared or a visible wave-front sensor, the latter leading to anisoplanetic conditions?

Our images of the Galactic Center region reveal more than forty individual sources. Down to a limit of $m_L = 11$, no source is detected at the location of Sgr A*.

Using a CFHT PUEO K-band image, we plotted colour-magnitude diagram (CMD) of all detected stars. We found that almost all types of stars previously identified in the region (AGB, LPV, WC9, WN9/WN10, Ofpe/WN9, YSO) form fairly homogeneous groups in this diagram. For some of the stars that were not previously classified, we propose an identification based on their location in the CMD. It shows that Ofpe/WN9 stars may be the major population of stars in the region.

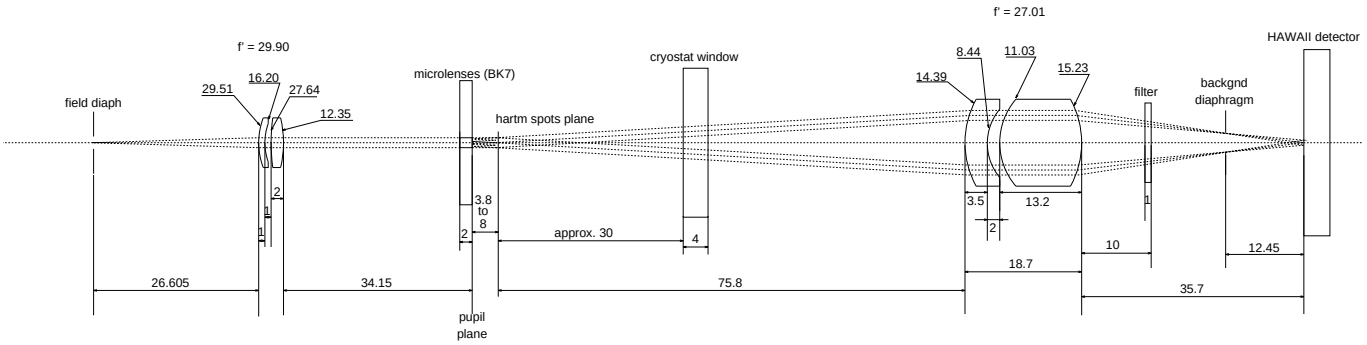

Fig. A.1. The beam comes from the ADONIS bench, on the left. The first element represented here is the field stop, with a diameter of 6 arcsec. Next, a collimator forms the pupil image on the microlenses. All these optical pieces are at ambiant temperature. Finally, a cold relay optics reimages the spots, with the appropriate magnification, on the detector. The filter is inside the cryostat.

Considering these bluer stars as the most relevant indicator for the absorption towards the center of the Galaxy, we find a K-band extinction of 2.7. This value is among the lowest given by previous authors. It would indicate that the larger values invoked elsewhere do not originate from interstellar extinction but from intrinsic or local properties, though an extinction law more suited to L-band could account for both a common K-band extinction coefficient of 3 and the very low colours of these bluer stars.

Acknowledgements. Authors are grateful to D. Rabaud and G. Rousset, from ONERA, and to F. Chazallet, from Shatki Inc., for their helpful involvment in the preparation of the RASOIR run. They also would like to thank the ESO 3.6 m telescope team for its assistance during the RASOIR set-up.

Appendix A: RASOIR

In the perspective of the infrared wave-front sensor (IRWFS) to be delivered in 2001 for the NAOS (Nasmyth Adaptive Optics System) on the VLT Melipal telescope, Observatoire de Paris and ONERA proposed to ESO to build a prototype IRWFS. Called RASOIR (Gendron 2001) and designed to operate on the ADONIS bench, it had to demontrate this concept.

Despite a first attempt made by Rigaut et al. (1992), no IRWFS had been successfully implemented, and astronomical wave-front sensing is still done at visible wavelengths. However several technical advances in infrared detectors technology (Hodapp et al. 1995) make IRWFS more attractive:

- a comparable read-out noise in visible and infrared wavelengths (down to 9 e^-);
- a reasonably high quantum efficiency ($\eta_{\rm IR} \approx 0.6$ whereas $\eta_{\rm VIS} \approx 0.9$);
- the line read-out mode of infrared detectors (compared to the frame read-out mode of the visible detectors), which allows a more flexible and a faster read-out of the array, and windowing around the reference;
- a wide spectral bandpass(0.8−2.5 μm).

The main scientific argument that pleads for IRWFS is the existence of several classes of objects with no or faint counterpart at visible wavelengths: stars older than M6, proto-stars embedded in a cocoon of gas and dust, old stellar populations, objects located in the Galactic plane, ...

RASOIR is a camera designed by the Observatoire de Paris and hosting a 1024×1024 HgCdTe FPA HAWAII infrared array from Rockwell. The liquid nitrogen cryostat is especially designed to be stiff and movable in almost all directions. The dedicated readout electronics has the capability of reading only selected areas on the array, corresponding to the Shack-Hartmann pupils images. Even in the double correlated sampling mode, a frame frequency as high as 120 Hz is reachable on the Hawaii array. The camera is installed on the ADONIS bench with few additionnal optical components to adjust the beam. The optical scheme is represented in Fig. A.1. The nominal configuration is a 7×7 subaperture Shack-Hartmannn, with 6×6 pixels per subaperture. Thus, only 42×42 pixels of one quadrant of the array is used. The wave-front sensing is done exclusively in K-band.

For our Galactic Center observations, IRS 7 ($m_K = 6.6$) was used as the reference star for the adaptive optics system. Being close to the limit magnitude of RASOIR, we were forced to use a low close-loop sampling frequency (from 40 to 60 Hz). The readout noise was about 50 e^- rms.

References

Abbott, D. C., & Conti, P. S. 1987, ARA&A, 25, 113
Allen, C. W. 1973, in Astrophysical Quantities, third edition (The Athlone Press, London & Atlantic Highlands)
Allen, D. A., Hyland, A. R., Longmore, A. J., et al. 1977, ApJ, 217, 108
Balick, B., & Brown, R. L. 1974, ApJ, 194, 265
Beuzit, J.-L., Demailly, L., Gendron, E., et al. 1997, ExA, 7, 285
Blum, R. D., DePoy, D. L., & Sellgren, K. 1995, ApJ, 441, 603
Blum, R. D., Sellgren, K., & DePoy, D. L. 1996, ApJ, 470, 864
Bouchet, P., Manfroid, J., & Schmider, F. X. 1991, A&AS, 91, 409
Cohen, M., Van der Hucht, K. A., Williams, P. M., & Thé, P. S. 1991, ApJ, 378, 302

Davidge, T. J. 1998, AJ, 115, 2374
Diolaiti, E., Bendinelli, O., Bonaccini D., et al. 2000, SPIE, 4007, 879
Doyon, R., Nadeau, D., Vallée, P., et al. 1998, SPIE, 3354, 760
Eckart, A., Genzel, R., Hofmann, R., Sams, B. J., & Taconni-Garman, L. E. 1995, ApJ, 445, L23
Evans, N. J., Blair, G. N., & Beckwith, S. 1977, ApJ, 217, 449
Evans, N. J., Beckwith, S., Brown, R. L., & Gilmore, W. 1979, ApJ, 227, 450
Evans, N. J., Mundy, L. G., Kutner, M. L., & DePoy, D. L. 1989, ApJ, 346, 212
Frogel, J. A., & Whitford, A. E. 1987, ApJ, 320, 199
Gendron, E. 2001, in preparation
Genzel, R., Hollenbach, D., & Townes, C. H. 1994, Rep. Prog. Phys., 57, 417
Genzel, R., Thatte, N., Krabbe, A., Kroker, H., & Tacconi-Garman, L. E. 1996, ApJ, 472, 153
Genzel, R., Eckart, A., Ott, T., & Eisenhauer, F. 1997, MNRAS, 291, 219
Genzel, R., & Eckart, A. 1999, in ASP Conf. Ser. 186, ed. H. Falcke, A. Cotera, W. J. Duschl, F. Melia, & M. J. Rieke
Ghez, A. M., Klein, B. L., Morris, M., & Becklin, E. E. 1998, ApJ, 509, 678
Hodapp, K.-W., Hora, J. L., Hall, D. N., et al. 1995, SPIE, 2475, 8
Johnson, H. L. 1966, ARA&A, 4, 193
Jones, T. J., Hyland, A. R., Wood, P. R., & Gatley, I. 1983, ApJ, 273, 669
Krabbe, A., Genzel, R., Eckart, A., et al. 1995, ApJ, 447, L95
Lacombe, F., Marco, O., Geoffray, H., et al. 1998, PASP, 110, 1087
Lai, O., Véran, J.-P., Rigaut, F., et al. 1997, SPIE, 2871, 859
Le Bertre, T. 1991, A&AS, 90, 105
Lebofsky, M. J., Rieke, G. H., & Tokunaga, A. T. 1982, ApJ, 263, 736
Lonsdale, C. J., Becklin, E. E., Lee, T. J., & Stewart, J. M. 1982, AJ, 87, 1819
Lutz, D., Feuchtgruber, H., Genzel, R., et al. 1996, A&A, 315, L269
Mc Gregor, P. J. 1994, PASP, 106, 508
Manchado, A., Pottasch, S. R., Garcia-Lario, P., Esteban, C., & Mampaso, A. 1989, A&A, 214, 139
Menten, K. M., Reid, M. J., Eckart, A., & Genzel, R. 1997, ApJ, 475, L111
Merrill, K. M., & Stein, W. A. 1976, PASP, 88, 874
Najarro, F., Krabbe, A., Genzel, R., et al. 1997, A&A, 325, 700
Narayan, R., Mahadevan, R., Grindlay, J. E., Popham, R. G., & Gammie, C. 1998, ApJ, 492, 554
Noguchi, K., Qian, Z., Wang, G., & Wang, J. 1993, PASJ, 45, 65
Nota, A., Pasquali, A., Drissen, L., et al. 1996, ApJS, 102, 383
Ott, T., Eckart, A., & Genzel, R. 1999, ApJ, 523, 248
Pasquali, A., Langer, N., Schmutz, W., et al. 1997, ApJ, 478, 340
Quataert, E., Narayan, R., & Reid, M. J. 1999, ApJ, 517, L101
Reid, M. J. 1993, ARA&A, 31, 345
Rieke, G. H., & Lebofsky, M. J. 1985, ApJ, 288, 618
Rieke, G. H., Rieke, M. J., & Paul, A. E. 1989, ApJ, 336, 752
Rigaut, F., Cuby, G. J., Caes, M., et al. 1992, A&A, 259, L57
Rigaut, F., Salmon, D., Arsenault, R., et al. 1998, PASP, 110, 152
Simons, D. A., & Becklin, E. E. 1996, AJ, 111, 1908
Stetson, P. B. 1987, PASP, 99, 191
Thé, P. S., Wesselius, P. R., & Janssen, I. M. H. H. 1986, A&AS, 66, 63
Werner, M. W., Becklin, E. E., Gatley, I., et al. 1979, MNRAS, 188, 463
Wynn-Williams, C. G. 1982, ARA&A, 20, 587